Intramolecular Electron Transfer in Cofacially π-Stacked Fluorenes: Evidence of Tunneling

Rajendra Rathore,*,† Sameh H. Abdelwahed,† Matthew K. Kiesewetter,‡ Richard C. Reiter,‡ and Cheryl D. Stevenson*,‡

Department of Chemistry, Illinois State University, Normal, Illinois 61790-4160, and Department of Chemistry, Marquette University, P.O. Box 1881, Milwaukee, Wisconsin 53201-1881

Received: May 24, 2005; In Final Form: November 18, 2005

The one-electron reduction of neutral π-stacked di- and trifluorenes (**F-2** and **F-3**) in HMPA, where ion association is absent, results in the formation of anion radicals in which the odd electron resides predominantly on just one of the external fluorene moieties, as established by EPR spectroscopy. However, in the case of tetrafluorene, introduction of a single electron leads to a kinetically controlled anion radical **F-4**$_{(int)}^{\bullet -}$ in which the odd electron undergoes rapid exchange between two central fluorene rings, where the anionic charge is partially shielded from solvation due to the presence of external fluorene rings. On a time scale of minutes, anion radical **F-4**$_{(int)}^{\bullet -}$ converts to a thermodynamically stabilized anion radical **F-4**$_{(ext)}^{\bullet -}$, with the electron exhibiting coupling from the protons on an external fluorene moiety. The charge and spin residing on an external moiety allow efficient solvation of the anionic charge. A similar fast exchange of a single electron (probably with the involvement of quantum mechanical tunneling) among three and four internal fluorene moieties is initially observed via EPR spectroscopy in the penta- and hexafluorene derivatives, **F-5** and **F-6**, respectively.

Introduction

Interactions between aromatic rings via π-stacking are the basis of many phenomena of organic material science and biological chemistry including the electron transport in DNA through π-stacked bases.[1] The quintessential example of the cofacial π-stacking phenomenon is represented by the cyclophanes, in which the two π-systems are forced into a sandwich-like geometry that generally enforces extensive cofacial aromatic conjugation.[2] In the paracyclophane radical anion, the unpaired electron displays complete delocalization through a nonclassically conjugated π-stack,[2] Figure 1. Since the electron is fully delocalized, EPR studies reveal that the odd electron is simultaneously in both ring systems and exhibiting hyperfine structure from eight ring protons.

Analogous systems, where the intramolecular electron exchange is on a subnanosecond time scale, but without full delocalization, are unknown. Such systems would probably involve quantum mechanical tunneling, and would not only allow the study of electron transport phenomenon through stacked aromatic moieties but would be of interest to those involved in the development of conducting "wire-like" molecules.[3] The involvement of quantum mechanical tunneling would necessarily perturb the spin−orbit coupling and hence the *g*-value, which determines the center field position of the EPR resonance. Analogous tunneling in inorganic systems is known to decrease the *g*-value,[4] and electron tunneling through cofacially π-stacked anion radicals should, likewise, decrease the observed *g*-value of the fast exchange resonances.

The recent availability of the π-stacked systems,[5] shown in Figure 2, coupled with EPR, which can be used to magnetically follow electrons, prompted us to explore the possibility of realizing one-electron tunneling through the cofacially π-stacked network.

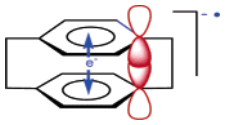

Figure 1. The π-stacked anion radical of paracylophane allowing *complete* conjugation of the added electron throughout both ring systems.

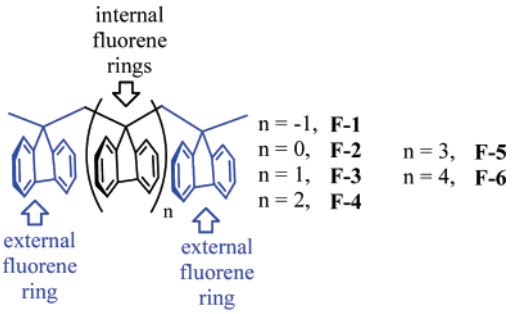

Figure 2. Structures and symbols for the cofacially π-stacked polyfluorenes used in this study.

Results and Discussion

The one-electron reduction of dimethylfluorene (**F-1**) in hexamethylphosphoramide (HMPA), where ion association is absent,[6] leads to the formation of the unassociated radical anion. EPR analysis reveals that the added electron is delocalized throughout the two-dimensional π-conjugated network, and it is interacting with all eight ring protons, Figure 3. The spectral pattern is nearly identical with that previously reported by

* Address correspondence to these authors. E-mail: cdsteve@ilstu.edu and rajendra.rathore@marquette.edu.
† Illinois State University.
‡ Marquette University.

10.1021/jp052737m CCC: $33.50
Published on Web 01/07/2006

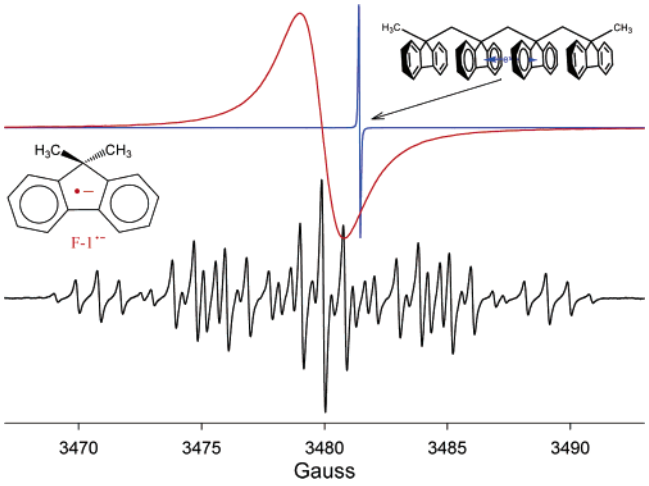

Figure 3. Ambient temperature EPR spectra of **F-1**$^{\bullet-}$ (lower), **F-1**$^{\bullet-}$ in the presence of 1 M neutral **F-1** (red), and **F-4**$_{(int)}^{\bullet-}$ (blue) all in HMPA. The resolved spectrum can be simulated by using a_H values of 5.2 G for 2Hs, 3.9 for 2Hs, and 0.9 G for 4Hs. The single line red spectrum is nicely simulated by using the same parameters but including a rate of electron exchange (reaction 1) of 1.2×10^8 M/s. The blue spectrum from **F-4**$^{\bullet-}$ reveals an extremely fast ($>10^{10}$) electron exchange between the two center fluorene moieties, which is *g*-shifted, probably due to the involvement of quantum mechanical tunneling.

Gerson et al. in a different solvent system.[2b] The addition of neutral **F-1** to this anion radical solution (ca. 1 M) results in fast electron exchange between the **F-1** radical anion and the **F-1** neutral molecule, reaction 1.

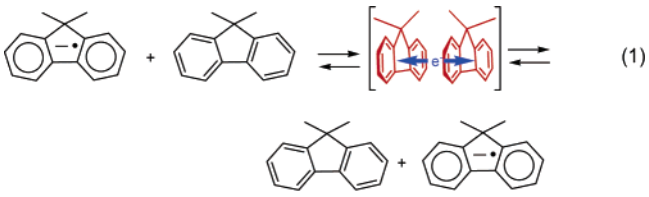

This encounter-controlled electron transfer (general transition state shown in structure **1**) severely limits the lifetime of the

1

individual radical anions. The resulting Heisenberg uncertainty in the resonance frequencies of the individual hyperfine components becomes so large that the well-resolved EPR pattern now appears as a single broad resonance with the same *g*-value[7] (red spectrum in Figure 3). Computer simulation reveals that the rate of electron exchange is 1.2×10^8 M/s, corresponding to an average lifetime for a radical anion of ca. 10^{-8} s. This single fast exchange EPR line grows narrower as the rate of exchange increases (via increasing the concentration of neutral **F-1** or increasing the temperature).[8] The reaction rate is, however, already near the encounter-controlled limit and the neutral molecule concentration is very large (1 M).

Unlike the case of **F-1**, the reduction of **F-4** leads to a greenish brown solution that initially exhibits only a single narrow line upon EPR analysis (blue spectrum in Figure 3).

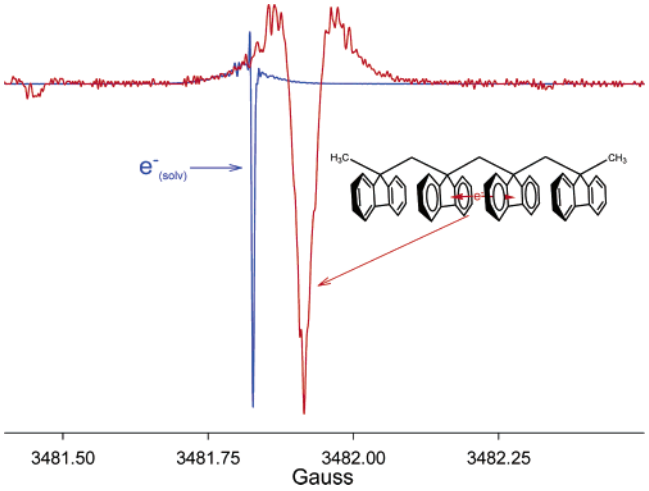

Figure 4. Second derivative X-band EPR signals from HMPA solutions of the solvated electron (blue) and from **F-4**$_{(int)}^{\bullet-}$ (red) obtained immediately after the reduction of **F-4**. Note that the signal from the solvated electron is much narrower and shifted downfield from that of **F-4**$_{(int)}^{\bullet-}$. The positions of the two resonances represent the averages of several recordings.

This single resonance is too broad ($\Delta w_{pp} = 0.06$ G) to be a result of solvated electron generated with alkali metal in HMPA; besides, it is present even when the number of added electrons is considerably smaller than the number of **F-4** molecules in solution. To eliminate any possibility that this resonance is from the solvated electron, we generated the solvated electron under identical conditions, using K and HMPA, and measured the relative *g*-values. The 0.06 G wide resonance from **F-4**$^{\bullet-}$ proved to be 0.088 G upfield of that due to the very narrow solvated electron (see Figure 4).

The 0.06 G wide resonance is a result of very rapid intramolecular electron exchange. The species responsible for the single resonance slowly decays while that due to **F-4**$^{\bullet-}$, with the odd electron located on an external fluorene moiety, grows in. After about 20 min, EPR analysis of the anion radical of **F-4** shows the simultaneous presence of two different species, one being that with a reduced external ring (**F-4**$_{(ext)}^{\bullet-}$) and the other exhibiting only the single sharp EPR resonance. **F-4**$_{(ext)}^{\bullet-}$ exhibits a_H values that are nearly identical with those for **F-1**$^{\bullet-}$. The species represented by the single fast exchange resonance is the anion radical of **F-4** but with the odd electron on the internal fluorene moieties (**F-4**$_{(int)}^{\bullet-}$). The electron is undergoing very rapid exchange between the two internal fluorene moieties. This exchange is so rapid that the resonance is in the extreme fast exchange condition.

Apparently, the kinetically controlled reduction product is **F-4**$_{(int)}^{\bullet-}$ while the thermodynamically controlled product is **F-4**$_{(ext)}^{\bullet-}$, and the half-life of **F-4**$_{(int)}^{\bullet-}$ in the reaction **F-4**$_{(int)}^{\bullet-}$ → **F-4**$_{(ext)}^{\bullet-}$ is tens of minutes, reaction 2. The long half-life of

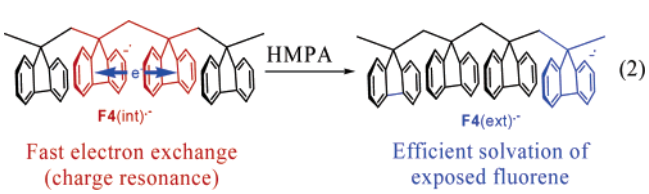

F-4$_{(int)}^{\bullet-}$ must mean that the anionic charge is significantly stabilized by fast electron exchange (or charge resonance) over two internal fluorene moieties (see reaction 2).[9a] Eventual formation of **F-4**$_{(ext)}^{\bullet-}$ occurs with the electron relocalization on one of the external fluorene moieties due to the stabilization

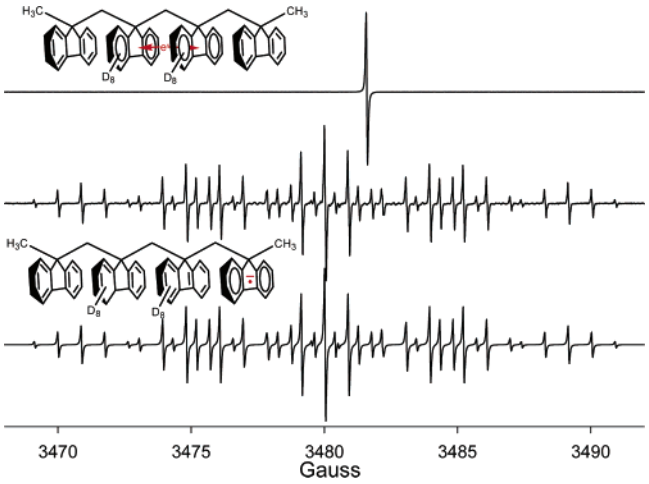

Figure 5. (Upper) Room temperature EPR spectrum obtained immediately after the one-electron reduction of **F-4-d**$_{16}$ in HMPA resulting in **F-4-d**$_{16(int)}^{\bullet-}$. The intense single line at 3481.9 G is due to an anion radical in which the spin is exchanging very rapidly between the 2nd and 3rd fluorene moieties. (Middle) The spectrum of the same solution, recorded 3 min later. **F-4-d**$_{16(ext)}^{\bullet-}$ is the only paramagnetic species observed. (Lower) A computer-generated simulation using a_H values of 0.88 G for 4Hs, 5.20 G for 2Hs, and 3.94 G for 2Hs ($\Delta w_{pp} = 0.045$ G). This clearly shows that the spectrum exhibiting proton hyperfine couplings is due to the electron located in an external fluorene moiety.

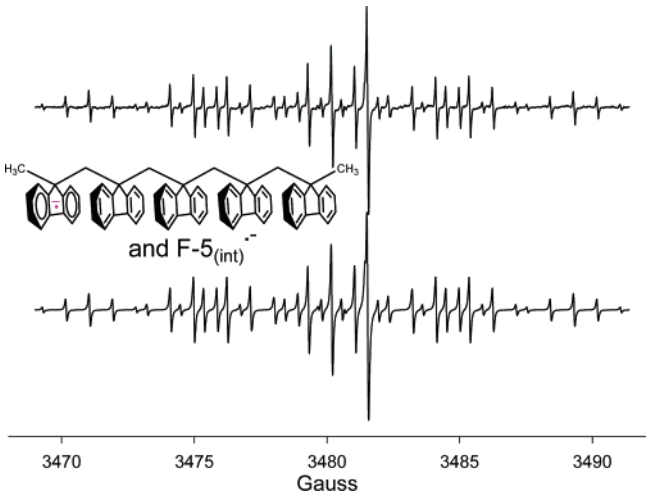

Figure 6. (Upper) The ambient temperature EPR spectrum of the HMPA solution of **F-5**, about 10 min after the potassium metal reduction. (Lower) A computer-generated simulation using a [**F-5**$_{(int)}^{\bullet-}$]/[**F-5**$_{(ext)}^{\bullet-}$] = 1/4 mixture and an exchange rate of ca. 10^{10} s^{-1} (for the internally reduced case). The spectrum due to the rapidly exchanging species is shifted 1.35 G upfield with respect to that of **F-5**$_{(ext)}^{\bullet-}$. The a_H values used are 0.88 G for 4Hs, 5.20 G for 2Hs, and 3.94 G for 2Hs along with a Δw_{pp} of 0.055 G.

of the anionic charge by an efficient solvation of the exposed fluorene moiety. The spin and charge relocalization must also be associated with a concurrent (unclear) structural change in the carbon backbone. If the above analysis is correct, the perdeuteriation of the two internal moieties should result in a nearly identical EPR pattern, with the line width of the fast exchange EPR line being different, reflecting the smaller deuterium couplings ($a_H/a_D = 6.49$), and any isotope effect upon the intramolecular electron-transfer kinetics.[9b−d]

The solution electron affinities of perdeuterated aromatic hydrocarbons are less than those of perprotiated hydrocarbons by about 0.5 kcal/mol.[9b−d] Hence, it might be anticipated that the rate of transformation from **F-4**$_{(int)}^{\bullet-}$ to **F-4**$_{(ext)}^{\bullet-}$ would be augmented via deuteriation of the central moieties. Indeed, the reduction of **F-4-d**$_{16}$ (deuteriation of the two internal moieties) gives a greenish brown solution yielding a single resonance upon EPR analysis due to **F-4-d**$_{16(int)}^{\bullet-}$ (Figure 5, upper). However, the resonance due to **F-4-d**$_{16(ext)}^{\bullet-}$ grows in at the expense of that for **F-4-d**$_{16(int)}^{\bullet-}$ in a matter of seconds. Hence, **F-4-d**$_{16(int)}^{\bullet-}$ → **F-4-d**$_{16(ext)}^{\bullet-}$ is at least an order of magnitude faster than the analogous reaction involving the perprotiated systems, Figure 5.

The single electron reduction of **F-2** (see Figure 2) with potassium metal in HMPA results in the formation of a greenish brown anion radical solution that yields an EPR pattern that is nearly identical with that for **F-1**$^{\bullet-}$. This implies that the spin (added electron) resides exclusively on only one ring of the **F-2** anion radical, and the presence of the unreduced ring does not significantly perturb the spin distribution in the reduced ring. There appears to be no communication between a reduced ring system and an adjacent unreduced ring. Further, the anion radical of **F-3** also yields nearly an identical EPR pattern, suggesting that 100% of the spin density is on one exterior ring system (**F-3**$_{(ext)}^{\bullet-}$). The solution electron affinity (EA) of the exterior fluorene moieties must be considerably larger than that of an interior fluorene moiety. In support of this interpretation, the one-electron reduction of **F-3-d**$_8$, where only the central fluorene moiety is deuterated, reveals an EPR pattern that is identical with that for perprotiated **F-3**$^{\bullet-}$. Noticeably absent in both the **F-2** and **F-3** anion radical systems is the fast intramolecular electron transfer observed in **F-4**$_{(int)}^{\bullet-}$. Apparently, the rapid exchange mechanism involves only multiple internal moieties. Hence, we anticipated fast exchange resonance(s) in the anion radical of **F-5**.

As in the case of **F-4**$^{\bullet-}$, rapid (on the EPR time scale) electron exchange in **F-5**$^{\bullet-}$ occurs only between internal rings. The initial EPR signal from **F-5**$^{\bullet-}$ reveals a single narrow fast exchange signal which, when greatly expanded at lower temperatures, appears to originate from more than one resonance, Figure 6. These resonances, most likely, arise from an exchange involving two and three internal fluorene moieties, respectively.

Similarly, a few minutes after the one-electron reduction of **F-6** (Figure 7), more than one fast exchange resonance is apparent along with those from the externally reduced system (**F-6**$_{(ext)}^{\bullet-}$), which displays the typical pattern observed for one reduced external fluorene ring system, Figure 8. The **F-6** system has two internal environments where rapid electron transfer can take place between two fluorene units, that is between the second and third moieties (**F-6**$_{2-3(int)}^{\bullet-}$) or between the third and fourth moieties (**F-6**$_{3-4(int)}^{\bullet-}$). However, examination of the fast exchange resonances reveals that there are at least three anion radicals undergoing rapid electron exchange. One of these displays a line width that is more than double that of the other two, suggesting that multiple central rings are involved. Presumably, **F-6**$_{2-5(int)}^{\bullet-}$ is thermodynamically favored (relative to the other F-6$_{(int)}^{\bullet-}$ systems) due to its more extended conjugation.

Notably, the "single" upfield resonance from the **F-5**$^{\bullet-}$ system does not exhibit observable temperature dependence down to 273 K. However, while HMPA freezes near 273 K, the addition of THF to the HMPA solutions allows EPR studies to be carried out at lower temperatures. At 262 K, the resonances are sufficiently narrow to clearly reveal two fast exchange resonances. Presumably, one is due to the exchange between the second and third fluorene rings, and the other is due to an exchange involving the three central fluorene moieties. The kinetics of transformation from the internal (rapidly exchanging) anion radical (i.e. **F-5**$_{(int)}^{\bullet-}$) to the species with the electron located on an external moiety (i.e. **F-5**$_{(ext)}^{\bullet-}$) is greatly dimin-

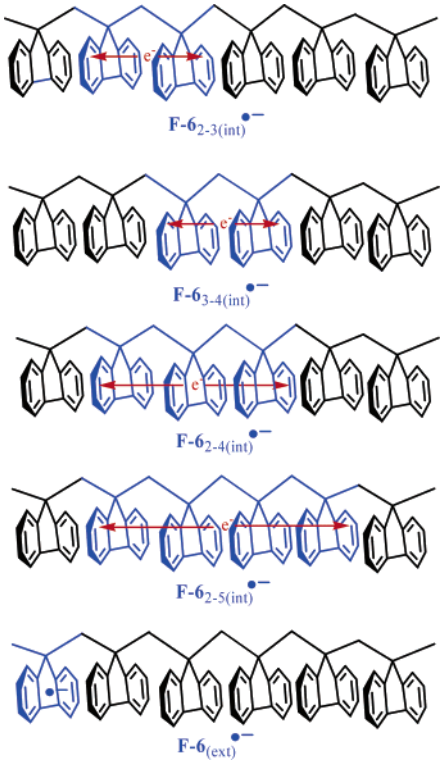

Figure 7. Various possible anion radical structures from the one-electron reduction of hexafluorene derivative **F-6**.

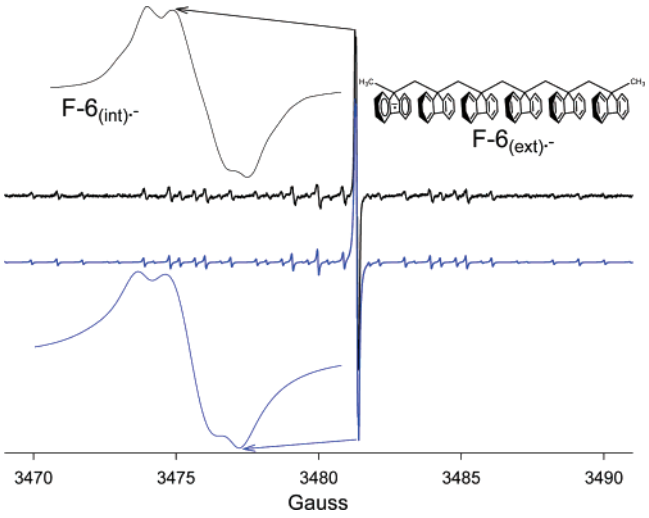

Figure 8. (Upper) The ambient temperature EPR spectrum of the HMPA solution of **F-6**, about 10 min after the potassium metal reduction. (Lower) A computer simulation using a mixture of anion radicals: [**F-6**$_{2-3(int)}^{\bullet-}$]/[**F-6**$_{3-4(int)}^{\bullet-}$]/[**F-6**$_{2-5(int)}^{\bullet-}$]/[**F-6**$_{(ext)}^{\bullet-}$] = 1/1/25/8. The exchange rates for **F-6**$_{2-3(int)}^{\bullet-}$ and **F-6**$_{3-4(int)}^{\bullet-}$ are about 10^{12} s^{-1}. The single EPR line representing **F-6**$_{2-5(int)}^{\bullet-}$ is twice as broad as the other two fast exchange resonances. (Inserts) Expanded views of the EPR signal (top) and simulation (bottom) of only the rapidly exchanging species (**F-6**$_{2-3(int)}^{\bullet-}$, **F-6**$_{3-4(int)}^{\bullet-}$, and **F-6**$_{2-5(int)}^{\bullet-}$) in the anion radical of **F-6**.

ished at the lower temperatures. This transformation takes place in minutes at ambient temperature and over a period of hours at 262 K.

The resonances due to the fast intramolecular electron transfer (or charge resonance) in the anion radicals of **F-4**, **F-5**, and **F-6**, Figures 3, 6, and 8, are all shifted upfield by more than a gauss, signifying that the *g*-values for these rapidly exchanging systems are less than those for the nonexchanging externally reduced rings by more than one part in 3000. This is a large

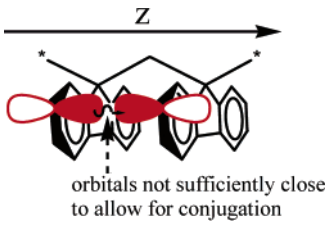

Figure 9. A depiction of two nearly overlapping p orbitals in adjacent fluorene systems. The p orbitals are not close enough to allow full delocalization, but the odd electron can rapidly translate through the narrow gap between them creating a fast (on the EPR time scale) electron exchange condition.

reduction in the *g*-value, which must arise from a perturbation in the spin−orbit coupling,[10] and (as has been known for almost a half century)[11] it cannot occur as a result of simple fast electron exchange. Since hyperfine structure from the internal rings is not observed, the spin−orbit coupling is not altered due to a simple extension of conjugation. Most likely, the proximity of the p_z orbitals (Figure 9) and consequent interaction (not simple conjugation) severely perturbs the orbital angular momentum of the unpaired electron. Therefore, we believe that quantum mechanical tunneling is involved. Analogous tunneling in solid inorganic systems is known to decrease the *g*-value,[4] and in the current case, electron tunneling through cofacially π-stacked anion radicals accounts for the observed decrease in the *g*-value of the fast exchange resonances. In these systems, the electron tunneling is perpendicular to the normal orbital angular momentum in the fluorenes. This, in turn, alters the spin−orbit coupling and hence the observed *g*-values.

Conclusions

In $CDCl_3$ solution, ^1H NMR spectroscopic data clearly established the rich cofacial π-stacking from the first fluorene to the last in the neutral **F-2** to **F-6** polyfluorene systems.[5] However, the one-electron reduction of π-stacked polyfluorenes in HMPA does not lead to full delocalization of the odd electron throughout all of the face-to-face fluorene moieties. Instead, in the thermodynamically preferred state, the spin density is located exclusively on one of the outer (or external) fluorene moieties. The initial, kinetically controlled reduction product, however, is one in which the p_z orbitals that make up the π-systems of the internal rings of the anion radicals of **F-4**, **F-5**, and **F-6** are sufficiently close to allow very rapid exchange of the odd electron between adjacent internal ring systems. This, in turn, allows the stabilization of the internal anion radicals by charge resonance over multiple fluorene rings[9a] (e.g., see Figure 7). Due to the stringent solvation requirements for the stabilization of anionic charge, the kinetically preferred internal anion radicals eventually transform into external anion radicals. There, the single electron resides exclusively on the outer fluorene moieties and is exposed to efficient solvation.

Experimental Section

The cofacially π-stacked polyfluorenes were synthesized as previously described.[5] A glass tube was charged with 0.1 mmol of a polyfluorene (**F-1** to **F-6** or their deuterated analogues) and sealed with fragile ends. This tube was then placed into bulb C of the Pyrex glass apparatus shown in the Figure 10. A small amount of potassium metal was placed into bulb A, which was then sealed at point E. The entire apparatus was evacuated, and the potassium metal was sublimed into bulb B to form a potassium mirror. Bulb A was sealed from the apparatus at point F. HMPA (4 mL) was distilled from a separate flask, containing

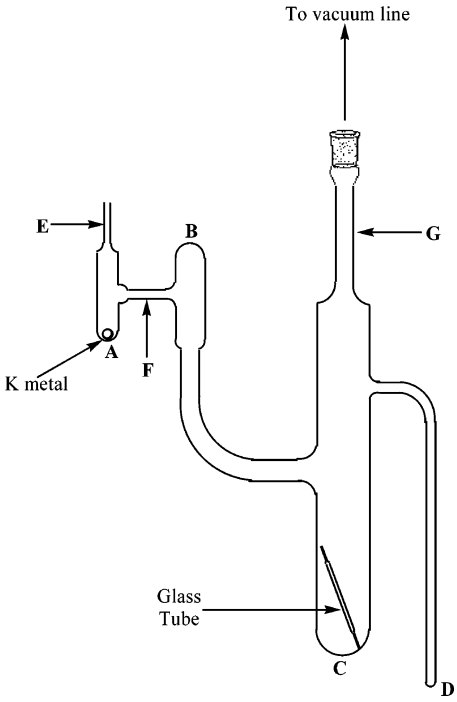

Figure 10. Apparatus used for the generation of the polyfluorene anion radicals.

potassium metal, directly into bulb C, and the evacuated apparatus was subsequently sealed from the vacuum line at point G. The apparatus was shaken vigorously to break the glass tube containing the polyfluorene and agitated lightly to dissolve it. The apparatus was then tilted to allow the solution to come into contact with the metal mirror until a dark green paramagnetic solution persisted. Initial reduction (short metal mirror−solution contact time) yields a transient paramagnetic green solution that quickly changes to a diamagnetic pink solution (anion radical disproportionation is presumably involved). Further reduction, however, results in a persistent green solution, which exhibits the strong single resonance (in **F-*n***, $n > 3$) upon EPR examination. This spectrum gradually evolves into a signal exhibiting proton hyperfine structure, as explained above.

The EPR spectrum was recorded immediately after reduction by placing the 3 mm tube D into the EPR cavity. The apparatus could be removed from the EPR spectrometer, the solution exposed to more metal, and the spectrum recorded again. This process was continued to allow monitoring of the EPR signal as a function of added metal. The simulations were carried out with the EWSIM software as previously described.[12] The difference between central EPR resonance positions observed for the anion radical systems exhibiting proton hyperfine structure (e.g., **F-5**$_{(ext)}^{\bullet-}$) and those exhibiting a fast exchange "collapsed" single resonance (e.g., **F-5**$_{(int)}^{\bullet-}$) are obtained from samples where both species are present simultaneously. Thus, the measured shift in resonance position results from an "internal standard", not from two different sample tubes (see Figures 6 and 8).

The *g*-value comparison experiments were carried out by reducing an HMPA solution of **F-4** with potassium metal and simultaneously reducing a sample of the HMPA in the absence of **F-4**. An EPR scan of the solvated electron solution, exhibiting an extremely narrow signal, was followed by a scan of the **F-4**$^{\bullet-}$ solution. This procedure was repeated several times to obtain the relative resonance positions ("chemical shifts") of the two signals. These spectra were obtained in the form of their second derivatives for unambiguous observation of spectral centers, Figure 3. In all cases we only report shifts in resonance positions (not absolute *g*-values).

Acknowledgment. C.D.S. thanks NSF and the Petroleum Research Fund (PRF), and R.R. thanks NSF for a career award and the PRF, administered by the American Chemical Society.

References and Notes

(1) For examples see: (a) Dohno, C.; Stemp, E. D. A.; Barton, J. K. *J. Am. Chem. Soc*. **2003**, *125*, 9586. (b) Treadway, C. R.; Hill, M. G.; Barton, J. K. *Chem. Phys.* **2002**, *2*−*3*, 409. (c) Lewis, F. D.; Miller, S. E.; Hayes, R. T.; Wasielewski, M. R. *J. Am. Chem. Soc*. **2002**, *124*, 11280.

(2) (a) Gerson, F.; Martin, W. B., Jr. *J. Am. Chem. Soc*. **1969**, *91*, 1883. (b) Gerson, F.; Kowert, B.; Peake, B. M. *J. Am. Chem. Soc*. **1974**, *96*, 118.

(3) (a) Ainsworth, S. J. *Chem. Eng. News* **2004**, *82(15)*, 17. (b) Baum, R. M. *Chem. Eng. News* **2004**, *82(15)*, 3.

(4) Coffman, R. E.; Lyle, D. L.; Mattison, D. R. *J. Phys. Chem*. **1968**, *72*, 1392.

(5) Rathore, R.; Abdelwahed, S. H.; Guzei, L. A. *J. Am. Chem. Soc.* **2003**, *125*, 8712.

(6) Ion association involving hydrocarbon anion radicals is absent in HMPA, see: (a) Levin, G.; Jagur-Grodzinski, J.; Szwarc, M. *J. Am. Chem. Soc*. **1970**, *92*, 2268. (b) Stevenson, C. D.; Echegoyen, L.; Lizardi, L. R. *J. Phys. Chem.* **1972**, *76*, 1439.

(7) Szwarc, M. In *Ions and Ion Pairs in Organic Reactions*; Szwarc, M., Ed.; John Wiley & Sons: New York, 1974; Vol. 2, p 61.

(8) Stevenson, C. D.; Rice, C. V. *J. Am. Chem. Soc*. **1995**, *117*, 10551.

(9) (a) Note that some anion radicals are known to associate with their neutral counterparts to form stabilized dimeric anion radicals, see: Ganesan, V.; Rosokha, S. V.; Kochi, J. K. *J. Am. Chem. Soc*. **2003**, *125*, 2559. (b) Stevenson, C. D.; Reidy, K. A.; Peters, S. J.; Reiter, R. C. *J. Am. Chem. Soc*. **1989**, *111*, 6578. (c) Stevenson, C. D.; Espe, M. P.; Reiter, R. C. *J. Am. Chem. Soc*. **1986**, *108*, 5760. (d) Hrovat, D. A.; Hammons, J. A.; Stevenson, C. D.; Borden, W. T. *J. Am. Chem. Soc*. **1997**, *119*, 9523.

(10) (a) Stone, A. J. *Mol. Phys.* **1963**, *6*, 509. (b) Segal, B. G.; Kaplan, M.; Fraenkel, G. K. *J. Chem. Phys.* **1965**, *43*, 4191. (c) Stevenson, C. D.; Kiesewetter, M. K.; Peters, S. J. *J. Phys. Chem. A* **2004**, *108*, 2278.

(11) Ward, R. L.; Weissman, S. I. *J. Am. Chem. Soc*. **1957**, *79*, 2086.

(12) (a) Morse, P. D., II; Reiter, R. C. *EWSIM*; Scientific Software Services: Plymouth, MI, 1992. (b) Zuilhof, H.; Lodder, G.; van Mill, R. P.; Mulder, P. J.; Kage, D. E.; Reiter, R. C.; Stevenson, C. D. *J. Phys. Chem.* **1995**, *99*, 3461. (c) For an example of this software used for line width modulation effects, see: Stevenson, C. D.; Kim. Y. S. *J. Am. Chem. Soc*. **2000**, *122*, 3211.